DOI: 10.1002/chem.200900548

Asymmetric Transfer Hydrogenation of Ketones Catalyzed by Amino Acid Derived Rhodium Complexes: On the Origin of Enantioselectivity and Enantioswitchability

Katrin Ahlford,[a] Jesper Ekström,[a] Alexey B. Zaitsev,[a] Per Ryberg,[b] Lars Eriksson,[c] and Hans Adolfsson*[a]

Abstract: Amino acid based thioamides, hydroxamic acids, and hydrazides have been evaluated as ligands in the rhodium-catalyzed asymmetric transfer hydrogenation of ketones in 2-propanol. Catalysts containing thioamide ligands derived from L-valine were found to selectively generate the product with an *R* configuration (95% *ee*), whereas the corresponding L-valine-based hydroxamic acids or hydrazides facilitated the formation of the (*S*)-alcohols (97 and 91% *ee*, respectively). The catalytic reduction was examined by performing a structure–activity correlation investigation with differently functionalized or substituted ligands and the results obtained indicate that the major difference between the thioamide and hydroxamic acid based catalysts is the coordination mode of the ligands. Kinetic experiments were performed and the rate constants for the reduction reactions were determined by using rhodium–arene catalysts derived from amino acid thioamide and hydroxamic acid ligands. The data obtained show that the thioamide-based catalyst systems demonstrate a pseudo-first-order dependence on the substrate, whereas pseudo-zero-order dependence was observed for the hydroxamic acid containing catalysts. Furthermore, the kinetic experiments revealed that the rate-limiting steps of the two catalytic systems differ. From the data obtained in the structure–activity correlation investigation and along with the kinetic investigation it was concluded that the enantioswitchable nature of the catalysts studied originates from different ligand coordination, which affects the rate-limiting step of the catalytic reduction reaction.

Keywords: amino acids · asymmetric catalysis · kinetics · reaction mechanisms · rhodium

Introduction

The asymmetric reduction of ketones to yield enantiomerically enriched secondary alcohols is a key transformation in numerous synthetic procedures leading to compounds with interesting biologically activity. One particularly attractive, mild, and highly selective method for ketone reductions is the asymmetric transfer hydrogenation (ATH) protocol.[1,2] In the ATH reaction, a prochiral ketone is selectively reduced by transfer of a hydride and a proton from a suitable hydride donor, most often mediated by a chiral transition-metal complex. When developing a catalytic system for the ATH reaction there are three major aspects to consider: 1) the choice of hydride donor, 2) the transition-metal source, and 3) the chiral ligand, which will enable the process to proceed with good stereoselectivity. There are in principle two different types of donors frequently used in the ATH reaction. These can be classified as either reversible or irreversible donors, with 2-propanol being the classic example of a reversible donor and formic acid a good example of an irreversible donors. The use of formic acid, alkali metal formate, or the triethylamine/formic acid (2:5) azeotrope (TEAF) is considered more advantageous because the

[a] K. Ahlford, Dr. J. Ekström, Dr. A. B. Zaitsev, Prof. Dr. H. Adolfsson
Department of Organic Chemistry, Stockholm University
The Arrhenius Laboratory, 10691 Stockholm (Sweden)
Fax: (+46) 8-154908
E-mail: hansa@organ.su.se

[b] Dr. P. Ryberg
Global Process R&D, AstraZeneca, 15185 Södertälje (Sweden)

[c] Dr. L. Eriksson
Department of Physical Chemistry, Inorganic Chemistry and Structural Chemistry
The Arrhenius Laboratory, 10691 Stockholm (Sweden)

Supporting information for this article is available on the WWW under http://dx.doi.org/10.1002/chem.200900548. Experimental procedures for ligand and complex formation, catalytic and kinetic experiments, and ligand characterization data.

resulting carbon dioxide formed after the hydride/proton transfer is thermodynamically much more stable, which makes the reaction almost completely irreversible. However, the downside is that only a narrow range of catalysts that tolerate the use of formic acid as the hydride donor are available. In contrast, ATH reactions performed under reversible conditions in secondary alcohols like 2-propanol can be catalyzed by a wider range of transition-metal complexes.[3] For an ATH process to favorably give the desired product under reversible conditions, the substrate needs to have an oxidation potential that differs from that of the hydride donor.[4] Even so, the donor needs to be present in large excess because the erosion of product enantioselectivity is often observed even if the equilibrium is in favor of the substrate. There are several metal sources available that have the ability to mediate the hydride transfer from the donor to the substrate. Even if main-group metals like aluminium have historically been used in the transfer hydrogenation reaction,[5–7] today's catalysts of choice are transition-metal complexes predominantly of ruthenium, rhodium, and iridium.[1] In addition, a few highly interesting reports describing the use of iron complexes have recently been published.[8] The most well-known and successful transition-metal complex used to catalyze the ATH reaction is unquestionably the Noyori catalyst (**1**), which is formed from [{$RuCl_2$(*p*-cymene)}$_2$] and the monotosylated 1,2-diphenyl-1,2-diaminoethane (TsDPEN).[1h,9]

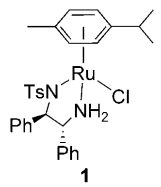

1

This particular complex shows high catalytic activity with both categories of hydride donors, and prochiral ketones as well as imines have successfully been reduced with high enantioselectivity in TEAF. In addition to **1**, ruthenium complexes of vicinal amino alcohols show high activity and often good-to-excellent selectivity in the reduction of ketones. However, these reactions only work properly with alcohols as the hydride donor.[10]

We and others have demonstrated that α-amino acids can serve as efficient ligand precursors to ATH catalysts.[11,12] The modular nature of α-amino acids make them highly attractive as ligand building blocks and a multitude of ligands with different structural features can easily be prepared and evaluated. We recently reported that ruthenium and rhodium complexes of *N*-carbamate-protected amino acid derivatives, pseudo-dipeptides (**2**), thioamides (**3**), and hydroxamic acids (**4**), successfully catalyze the ATH reactions of aryl alkyl ketones with high activity and excellent enantioselectivity.[11]

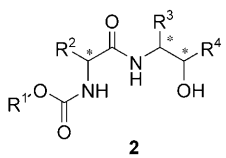
2

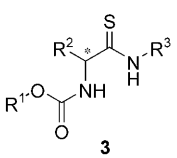
3

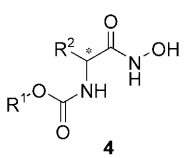
4

These catalytic systems behave in accordance with amino alcohol systems and only show activity with alcohols as hydride donors. When we investigated the catalytic activity and selectivity of Ru/Rh complexes composed of the different ligands **2**–**4** in the ATH reactions of acetophenone, we obtained a most interesting result. By using ligands made from natural (*S*)-amino acids, we found that catalysts derived from pseudo-dipeptides (**2**) and hydroxamic acids (**4**) selectively catalyzed the formation of the (*S*)-alcohol,[11a–f,h] whereas complexes derived from the corresponding thioamide ligands (**3**) gave the product with the *R* configuration.[11g] Hence, the same amino acid scaffold can evidently be used for the construction of catalysts that selectively favor the formation of either of the product enantiomers, simply by changing the nature of the amino acid C terminus. Herein we present results that serve to further our understanding of the reasons behind the observed enantioswitchability when catalysts derived from **2**–**4** are used in the ATH reactions of ketones in 2-propanol.

Results and Discussion

In our previous studies on the use of pseudo-dipeptides (**2**) as ligands for ruthenium and rhodium in the ATH reaction we were neither able to isolate nor obtain sufficient spectroscopic data to be able to conclude the structure of the precatalyst or the active catalyst. Nevertheless, by using chemical methods we found that the nature of the ligands' functional groups was strongly correlated to the activity and selectivity of the catalysts.[11b] In fact, most changes made to the structure of **2** led to a significant decrease in the catalytic activity. We found that it is essential that the N terminus of the ligand is "protected" as a base-stable carbamate because catalysts formed with ligands containing either carboxamides, sulfonamides, or simply unprotected amines gave no conversion to the product. The peptide bond, referred to as the central amide, that is formed upon coupling of the 1,2-amino alcohol to the amino acid proved to be essential for catalytic activity. If the central amide was formed from a secondary amine, hence creating a tertiary amide, the catalytic activity was lost. The alcohol functionality at the C terminus of the pseudo-dipeptide was equally important for the activity of the catalyst, and when this group was converted into the corresponding methyl ether, no product formation was detected in the catalytic reduction. In addition, optimization studies of the catalytic reduction of acetophenone in 2-propanol using **2** and [{$RuCl_2$(*p*-cymene)}$_2$] showed that good activity was obtained with a base/ligand ratio of >3:1. The common feature of the working ligands is the presence of three acidic sites, which could explain the necessity of using a minimum of 3 equiv of sodium hydroxide or 2-propoxide. In most cases the pseudo-dipeptides studied contained two stereogenic centers and from the reaction outcome we found a good correlation between the stereocenter of the amino acid part of the ligand and the absolute configuration of the product obtained in the ATH reaction. Evi-

dently the chiral induction originated primarily from the amino acid and the stereocenter present in the amino alcohol part played a secondary role. Based on these data we concluded that the metal most likely interacts with all of the available functional groups in the pseudo-dipeptide ligand, however, the exact structure could not be elucidated. The problems encountered when trying to isolate a metal complex containing ligand **2** led to further structural variations. We argued that higher complex stability could be obtained by converting the central amide of the ligand into its corresponding thioamide, thereby increasing the acidity of this functionality.[13] To our surprise we found that this modification led to a ligand class with significantly different properties. In the ruthenium-catalyzed ATH reaction of acetophenone using a thioamide derived from a natural amino acid pseudo-dipeptide, we unexpectedly obtained the product with the opposite configuration.[11g] After catalyst optimization we discovered that the use of rhodium was superior to ruthenium and that the alcohol moiety of the ligand was redundant. Thus, the most efficient and selective catalyst was obtained from ligand **3a** ($R^1 = t$Bu, $R^2 = i$Pr, $R^3 = (S)$-CHPhCH$_3$) and [{RhCl$_2$Cp*}$_2$].[14] The observed switch in enantioselectivity on going from *N*-Boc-protected pseudo-dipeptides to thioamides was rather intriguing and we therefore decided to further elaborate the ligand structure to clarify the origin of this effect. The increased acidity of the thioamide could of course be one of the reasons for the switch in enantioselectivity. A similar outcome of the ATH reaction was therefore anticipated for an amino acid with the C terminus transformed into a hydroxamic acid. The ATH reactions of ketones with rhodium complexes of the hydroxamic acid ligands **4** derived from natural amino acids resulted in the selective formation of the (*S*)-alcohol, in agreement with the use of pseudo-dipeptide ligands. Clearly the observed enantioswitch is not connected to the acidity of the amide functionality, but possibly rather an effect of different modes of ligand coordination. To obtain data on the ligand mode of coordination, and thereby an insight into the origin of the enantioswitch observed, a catalyst structure–activity correlation investigation was performed. Hence structural variations were made to the amino acid derived thioamides and hydroxamic acids and the ligands were evaluated in the ATH reaction by using acetophenone as the model substrate.

Thioamide ligands derived from α-amino acids: In our previous study on the development of α-amino acid thioamide ligands for the ATH reaction of prochiral ketones, ligand optimization revealed that valine-derived **3a** in combination with [{RhCl$_2$Cp*}$_2$] gave the best catalytic activity and selectivity.[11g] Thus, the use of catalyst Rh–**3a** for the reduction of acetophenone resulted in high conversion and good enantioselectivity of the (*R*)-alcohol (Table 1, entry 1). When the reaction was performed with LiCl as an additive, an even higher *ee* was obtained (entry 2). Ligands based on other amino acids as well as on different amines were also investigated, but in all cases inferior results were obtained. Interestingly, when the diastereomeric ligand **3b** was used in the catalytic reduction, the same product isomer was obtained with good *ee* values (entries 3 and 4). Intrigued by these results we prepared compounds **3c** and **3d** and evaluated their performance in the ATH reaction. From the results presented in Table 1 (entries 5–8) it is clear that the presence of the isopropyl group in the amino acid is essential for the enantioselectivity and that the stereocenter in the amine part of the ligand is of less importance. We then turned our attention towards the N terminus of the ligand. Replacing the carbamate by an acetamide (**3e**) resulted in lower activity and selectivity of the reduction reaction (entries 9 and 10), whereas the use of ligand **3f** practically gave no conversion (entries 11 and 12). When ligand **3g** was employed in the ATH reaction of acetophenone we achieved good activity, albeit with significantly lower enantioselectivity (entry 13). Interestingly, when the reaction was performed in the presence of LiCl, no significant improvement in the enantiose-

Table 1. Rhodium-catalyzed ATH reaction of acetophenone using thioamide ligands.[a]

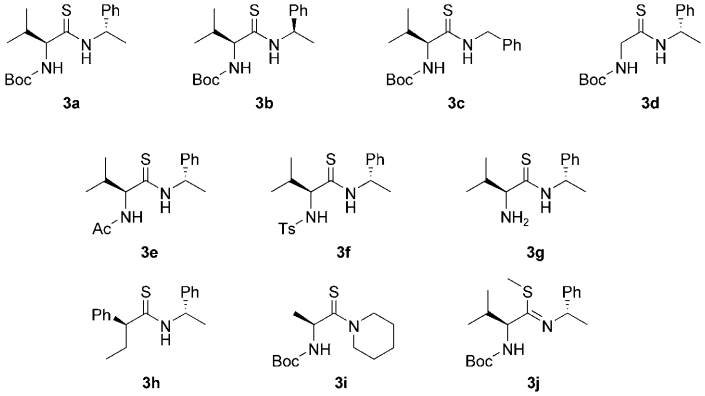

Entry	Ligand	Conversion [%][b]	Enantioselectivity [%][c]
1	**3a**	91	86 (*R*)
2[d]	**3a**	88	95 (*R*)
3	**3b**	72	88 (*R*)
4[d]	**3b**	87	89 (*R*)
5	**3c**	64	85 (*R*)
6[d]	**3c**	67	86 (*R*)
7	**3d**	31	4 (*R*)
8[d]	**3d**	43	9 (*R*)
9	**3e**	20	62 (*R*)
10[d]	**3e**	24	63 (*R*)
11	**3f**	1	–
12[d]	**3f**	2	–
13[e]	**3g**	82	47 (*R*)
14[d,e]	**3g**	65	49 (*R*)
15	**3h**	–	–
16[f]	**3i**	2	–
17	**3j**	–	–

[a] Reaction conditions: Acetophenone (1 equiv, 0.2 M in 2-propanol), [{RhCl$_2$Cp*}$_2$] (0.25 mol%), ligand (0.55 mol%), and 2-PrONa (5 mol%), 2 h, room temperature. [b] The conversion was determined by GLC analysis. [c] The enantiomeric excess was determined by GLC analysis (CP Chirasil DEXCB). [d] LiCl (5 mol%) was added to the reaction mixture. [e] Reaction time: 15 min. [f] [{RuCl$_2$(*p*-cymene)}$_2$] (0.5 mol%) was used as the metal precursor.

lectivity was observed (entry 14). The catalyst derived from ligand **3h**, which lacks the N terminus, was completely inactive. When the structure of the C terminus of the ligand was varied, we found that the catalyst formed with thioamide **3i**, derived from the corresponding tertiary amide, was essentially inactive (entry 16). The same result was obtained with the methylated thioamide **3j** (entry 17). Evidently, in agreement with our previous observations using pseudo-dipeptide ligands, it is of the utmost importance for the catalytic activity that the amide in the ligand can be deprotonated. To conclude, the structural features of the ligands that lead to active and stereoselective thioamide-based rhodium catalysts appear to be 1) steric bulk at the α position of the amino acid, 2) a carbamate protecting group at the N terminus, and 3) a removable proton at the C terminus.

Hydroxamic acid ligands derived from α-amino acids: The ATH reactions of acetophenone using rhodium catalysts based on the *N*-Boc-protected amino acid derived hydroxamic acid ligands **4a–c** resulted in good conversions and good-to-excellent enantioselectivity of 1-phenylethanol (Table 2, entries 1–6). In agreement with the reaction outcomes using pseudo-dipeptide catalysts, and in contrast to the corresponding thioamide-based catalysts presented above, we obtained the *S*-configured secondary alcohol as the major enantiomer. To further our understanding of the role and importance of the different functionalities present in the hydroxamic acids regarding catalytic activity and mode of coordination we decided to examine a number of structurally related ligands. The combination of $[\{RhCl_2Cp^*\}_2]$ and ligand **4d**, in which the Boc group is removed, resulted in decreased catalytic activity and selectivity (entries 7 and 8). The catalytic reduction of acetophenone using ligand **4e** containing a Cbz group at the N terminus gave a result similar to the corresponding Boc-protected ligand (entries 9 and 10), whereas catalysts derived from ligand **4f** or **4g** showed poor activity and selectivity (entries 11–14). Interestingly, the sulfonamide-containing ligand **4f** apparently induces the formation of the (*R*)-alcohol, even if the selectivity is poor. As in the case of the corresponding thioamide ligand, the use of compound **4h**, which completely lacks coordinating ability with anything but the hydroxamic acid, gave practically no product formation (entry 15). From the above results it is evident that the optimal amino acid derived hydroxamic acid ligand contains a carbamate protecting group at the N terminus because ligands with other functionalities gave no or poor performance. Next we focused on the catalytic activity of ligands with structural variation around the hydroxamic acid functionality. We prepared compounds **4i** and **4j** from *N*-Boc-valine and the corresponding monomethylhydroxylamines. Employing these and the commercially available **4k** as ligands in the rhodium-catalyzed ATH reaction of acetophenone resulted in overall poor activity. However, the enantioselectivity was significantly higher using compound **4j** than with the other two methylated hydroxamic acids (entries 16–21). These results indicate that the possibility of removing a proton from the nitrogen atom in the hydroxamic acid leads to a more selective catalyst.

Table 2. Rhodium-catalyzed ATH reaction of acetophenone using hydroxamic acid ligands.[a]

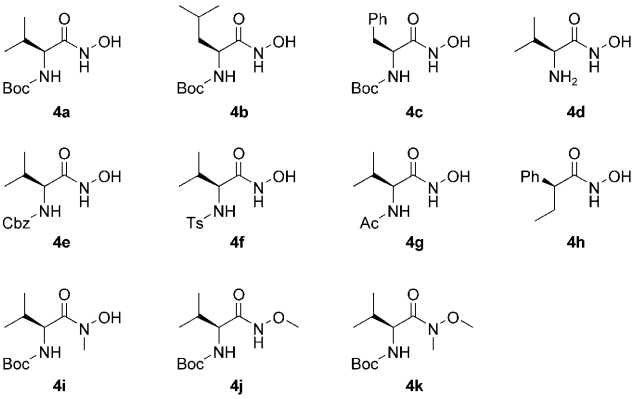

Entry	Ligand	Conversion [%][b]	Enantioselectivity [%][c]
1	**4a**	89	87 (*S*)
2[d]	**4a**	82	97 (*S*)
3	**4b**	43	89 (*S*)
4[d]	**4b**	62	95 (*S*)
5	**4c**	45	86 (*S*)
6[d]	**4c**	63	92 (*S*)
7	**4d**	43	33 (*S*)
8[d]	**4d**	47	34 (*S*)
9	**4e**	76	90 (*S*)
10[d]	**4e**	80	92 (*S*)
11	**4f**	2	–
12[d]	**4f**	8	53 (*R*)
13	**4g**	1	–
14[d]	**4g**	2	–
15	**4h**	4	–
16	**4i**	–	–
17[d]	**4i**	2	–
18	**4j**	16	70 (*S*)
19[d]	**4j**	10	36 (*S*)
20	**4k**	8	5 (*S*)
21[d]	**4k**	11	18 (*S*)

[a] Reaction conditions: Acetophenone (1 equiv, 0.2 M in 2-propanol), $[\{RhCl_2Cp^*\}_2]$ (0.25 mol%), ligand (0.55 mol%), and 2-PrONa (5 mol%), 2 h, room temperature. [b] The conversion was determined by GLC analysis. [c] The enantiomeric excess was determined by GLC analysis (CP Chirasil DEXCB). [d] LiCl (5 mol%) was added to the reaction mixture.

Hydrazide ligands derived from *N*-Boc-protected α-amino acids: As demonstrated by the results presented above using amino acid thioamide or hydroxamic acid ligands in the rhodium-catalyzed ATH reactions of ketones, the observed enantioswitch appears to be decoupled from the acidity of the functionality present at the ligand C terminus. This is further stressed by the fact that using *N*-Boc-L-valine as the ligand with $[\{RuCl_2(p\text{-cymene})\}_2]$ for the reduction of acetophenone resulted in the formation of the *S* enantiomer, although in poor conversion and enantioselectivity.[10g] Nevertheless, we decided to investigate the catalytic activity and selectivity by using an additional C terminus functionality. Amino acid hydrazides **5a–d** were efficiently prepared from *N*-Boc-protected alanine or valine and the corresponding *N*-

substituted hydrazines. Screening these compounds as ligands in the rhodium-catalyzed ATH reaction of acetophenone resulted in general in modest selectivity and conversions of up to 56% after 2 h. However, the catalyst formed with **5b** gave rather good enantioselectivity (Table 3, entry 4). Interestingly, in contrast to the pseudo-dipeptide thioamide or hydroxamic acid systems, the rhodium catalysts derived from hydrazide ligands showed catalytic activity even after a prolonged reaction time. Performing the rhodium-catalyzed reduction of acetophenone using ligand **5b** resulted in 67% conversion with maintained enantioselectivity (91%) after 4.5 h.

Table 3. Rhodium-catalyzed ATH reaction of acetophenone using hydrazide ligands.[a]

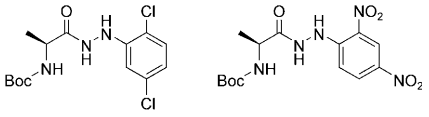

5a **5b**

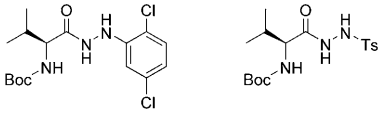

5c **5d**

Entry	Ligand	Conversion [%][b]	Enantioselectivity [%][c]
1	**5a**	43	80 (*S*)
2[d]	**5a**	9	49 (*S*)
3	**5b**	30	81 (*S*)
4[d]	**5b**	56	91 (*S*)
5	**5c**	20	84 (*S*)
6[d]	**5c**	7	50 (*S*)
7	**5d**	9	28 (*S*)
8[d]	**5d**	5	11 (*S*)

[a] Reaction conditions: acetophenone (1 equiv, 0.2 M in 2-propanol), [{$RhCl_2Cp^*$}$_2$] (0.25 mol%), ligand (0.55 mol%), and 2-PrONa (5 mol%), 2 h, room temperature. [b] The conversion was determined by GLC analysis. [c] The enantiomeric excess was determined by GLC analysis (CP Chirasil DEXCB). [d] 5 mol% of LiCl was added to the reaction mixture.

Catalyst structure: A comparison of the possible theoretical coordination modes of amino acid derived thioamides and hydroxamic acids revealed that these ligands can interact with the metal center in a number of different ways (Figure 1). As with the pseudo-dipeptides, the ATH reactions with ligands **3** and **4** require a certain amount of base to work properly (see below). We can therefore predict that the thioamide and the hydroxamic acid ligands will be ionized upon metal coordination. Hence, the possible modes of coordination of the thioamides can be visualized to be **I**–**V** in Figure 1 and for the hydroxamic acids to be **VI**–**X**.[15]

From the above presented structure–activity correlations using differently functionalized thioamides and hydroxamic acids, the following conclusions can be drawn regarding an individual ligand's mode of coordination. For the amino acid thioamides, the best catalytic activity and enantioselectivity was obtained by using the rhodium complex of ligand **3a**. Structural variations, including the removal of the *N*-Boc protecting group, changing it to either a carboxamide or a sulfonamide, or the use of a ligand completely lacking the N terminus, led invariably to less active and selective catalysts. Furthermore, *S*-alkylation of the thioamide or the use of a ligand containing a tertiary amide was equally ineffective. These observations indicate that the successful ligand coordinates to the rhodium center through the carbamate and the deprotonated thioamide. Hence, the most likely mode of coordination of the amino acid thioamide ligands is shown in structure **I** or **II** in Figure 1, although the soft nature of sulfur atom favors coordination mode **I**. The formation of complexes of the type **III** and **IV** cannot be completely excluded, although the larger seven-membered chelates formed in these cases should be thermodynamically less favored. The corresponding structure–activity investigation performed with the amino acid hydroxamic acids indicates that this class of ligand interacts with the metal center by chelation with the carbamate and most likely the nitrogen atom of the hydroxamic acid (i.e., coordination modes **VI** or **VIII** in Figure 1). For the same reason as given above for complexes **III** and **IV**, the interaction between the ligand and the metal according to **VIII** should be less energetically favored.

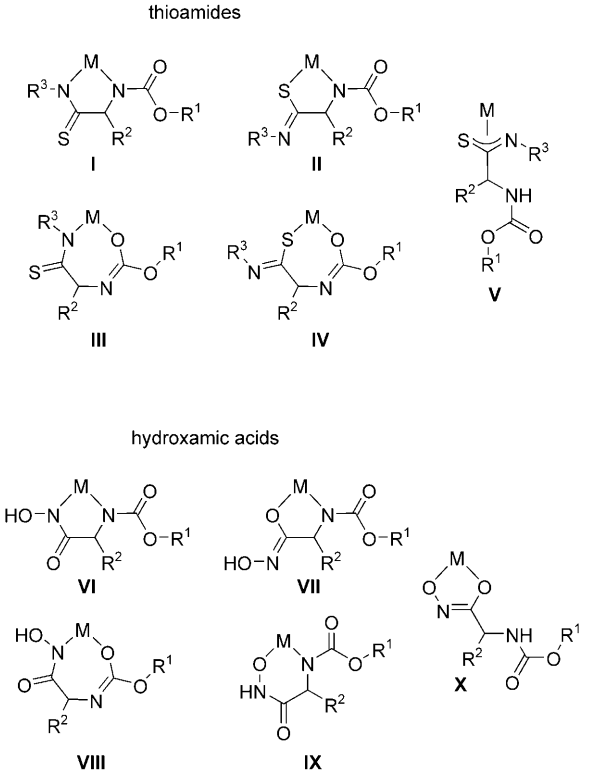

Figure 1. Possible modes of coordination of amino acid derived thioamides and hydroxamic acids.

The obvious approach for obtaining further structural knowledge of these complexes would be the use of spectroscopic or crystallographic methods. Therefore, rhodium–

arene complexes of the thioamide and hydroxamic acid ligands were synthesized. In separate reaction vessels, ligands ***ent*-3a** and ***ent*-4a** were treated with an excess of sodium hydride in dry dichloromethane, after which 1 equiv of $[\{RhCl_2Cp^*\}_2]$ was added. The resulting solutions were slowly evaporated to yield microcrystalline materials that could be isolated. In the case of the thioamide ligand, the crystals obtained were submitted to X-ray diffraction analysis, which yielded the structure presented in Figure 2.[16,17]

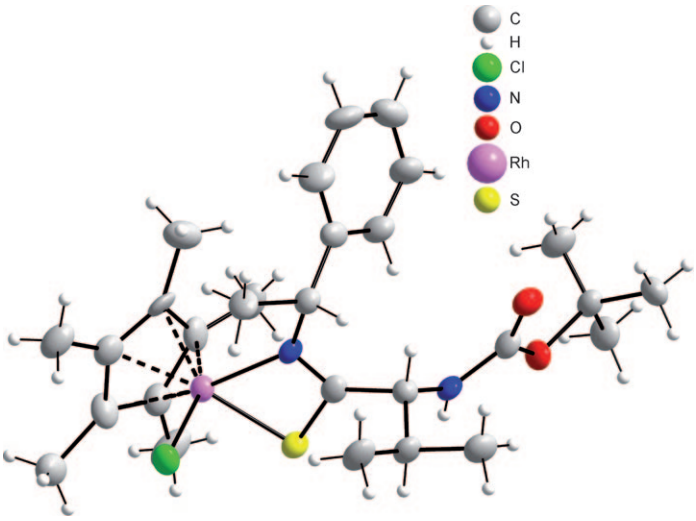

Figure 2. Molecular structure of the complex formed between ligand **ent-3a** and $[\{RhCl_2Cp^*\}_2]$.

The structure of the isolated complex shows that the ligand coordinates to the metal in a bidentate fashion, and much to our surprise, with the nitrogen and the sulfur atoms of the thioamide group (i.e., coordination mode **V** in Figure 1). Furthermore, when the isolated complex was employed as a precatalyst in the ATH reaction of acetophenone using the standard conditions (Table 1), the corresponding secondary alcohol was formed in moderate conversion (77% after 2 h), but with exceptionally poor enantioselectivity (17% in favor of the *S* isomer). Clearly the isolated complex is different from the active catalyst formed in situ between ligand **3a** and $[\{RhCl_2Cp^*\}_2]$. Because the isolated rhodium compound is the result of complex formation occurring under thermodynamic conditions, this particular structure does not necessarily mirror the actual structure of the active catalyst or the precatalyst operating in the ATH reaction. In fact, upon closer examination of the reaction profile obtained by using the thioamide-derived catalyst, deviation from the expected exponential behavior was observed (see below). Unfortunately, all attempts to isolate and characterize the corresponding complex of the hydroxamic acid ligand **4a** failed. In fact, the microcrystalline material that was isolated from the complex formation reaction turned out to be the $[\{RhCl_2Cp^*\}_2]$ starting complex. This finding indicates that the catalytically active rhodium complexes formed with hydroxamic acid ligands have rather weak ligand–metal interactions. To rule out the possibility that dimeric catalysts are operating in the reduction, we performed a nonlinear-effect study. The ATH reaction was executed with varying degrees of enantiomeric excess of catalyst Rh–**4a** by using the corresponding ligand ***ent*-4a** and the results obtained showed that the product *ee* was directly proportional to the stereochemical purity of the catalyst. The same analysis was performed by using catalyst Rh–**3a** and ***ent*-3a**, which displayed identical behavior. The linear dependence of the systems indicates that monomeric complexes are operating and hence the coordination models depicted in Figure 1 can be used to decipher the correct catalyst structure.

Reaction conditions: The standard reaction set-up for the ATH reactions presented above involves 0.25 mol% of the rhodium precursor, 0.55 mol% of the ligand, and 5 mol% of sodium isopropoxide. We had previously noticed that the amount of base is crucial for the catalytic activity of the systems under study. For instance, in the pseudo-dipeptide catalyst system a minimum base-to-catalyst ratio of 3:1 was required for the reduction to proceed.[11b] A lower amount of base resulted in no reaction, however, higher base ratios were tolerated and good conversion and excellent enantioselectivity were obtained even with 20 mol% of sodium isopropoxide (base/catalyst, 20:1). For the thioamide ligand system we found that the optimal amount of sodium isopropoxide was 10 mol% (10:1 ratio) and the highest conversions were achieved when the base was added subsequent to all other components, including the substrate.[11g] At lower base-to-catalyst ratios, the reaction rate was substantially decreased. The amino acid based hydroxamic acid ligand system was investigated in more detail and we found that the best base-to-metal ratio appeared to be 7:1. As can be seen in Figure 3, the use of less sodium isopropoxide result-

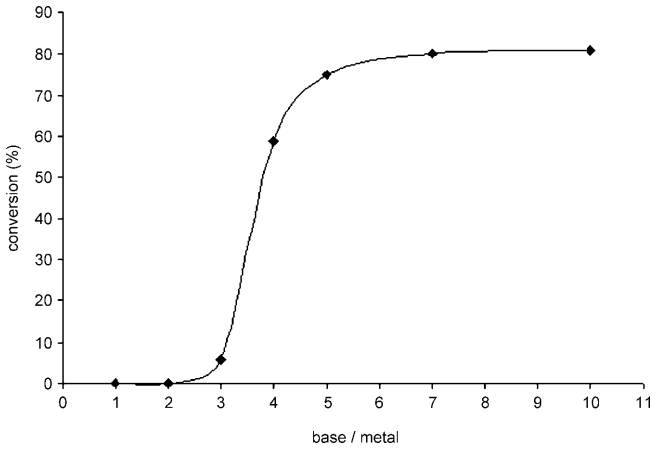

Figure 3. Effect of the sodium isopropoxide-to-catalyst ratio on the ATH reduction of acetophenone using $[\{RhCl_2Cp^*\}_2]$ and ligand **4a**. The conversion was monitored after 2 h.

ed in lower conversion, and a higher ratio did not result in a better reaction outcome. The enantioselectivity was not affected by the amount of base and in all the reactions in which we observed product formation, the *ee* of 1-phenylethanol was above 85%.

The observation that ruthenium-catalyzed transfer hydrogenation processes in 2-propanol are accelerated in the presence of base was made by Chowdhury and Bäckvall[18] in 1991, and most ATH protocols developed since then have shown similar behavior. Depending on the metal precursor used, the added base plays different roles.

When Ru–arene or Rh–Cp* catalyst precursors are employed, the dominant role of the base is to assist in the complex formation, often by ligand deprotonation. In all of the ligand systems described above there are at least two acidic sites that could be deprotonated by the base. The fact that higher sodium isopropoxide concentrations resulted in better and faster conversions indicates that the base is involved in additional processes.[18,19]

Effect of additives: In the asymmetric transfer hydrogenation reactions using ruthenium catalysts formed with pseudo-dipeptide ligands, we observed that the addition of lithium salts to the catalytic reaction had a beneficial effect on the product formation and the enantioselectivity.[11f] Alkali ions were found to be crucial for the catalytic turnover and reactions performed with additives such as crown ethers, which efficiently complex such metals, resulted in a significant drop in activity and selectivity. Moreover, DFT calculations indicated that the alkali ion is involved in the hydride transfer step by coordinating to the substrate and part of the catalyst. This coordination results in a highly organized transition state. In line with the experimental findings, we found that the presence of the smaller lithium ion resulted in the tightest TS, which naturally resulted in the highest selectivity. When we examined the influence of lithium additives on the corresponding rhodium pseudo-dipeptide catalytic system we found, to our surprise, that no such enhancing effect was obtained. Instead of an increase in the enantioselectivity, we achieved slightly lower *ee* values. As seen in Tables 1–3, the addition of lithium chloride had a beneficial effect on the product enantioselectivity in all of the catalyst systems studied. The most dramatic effects, an *ee* increase of around 10%, were obtained with the best ligands in each class (i.e., **3a**, **4a**, and **5b**). To rule out the possibility that the observed increase in *ee* was a result of added chloride, we performed the ATH reaction with hydroxamic acid ligand **4a** and [{$RhCl_2Cp^*$}$_2$] in the presence of a silver salt. The addition of silver triflate did not affect the enantioselectivity of the reaction because the product was obtained in 91% *ee* after 2 h (no LiCl present). Furthermore, we found that the addition of 10 mol% 15-crown-5 to the standard reaction set-up (with sodium isopropoxide as base) resulted in a decrease in conversion (45%) and selectivity (76% *ee*). The reaction can be performed with lithium isopropoxide as base, which results in the same outcome as the use of a mixture of the sodium base and lithium chloride. However, for practical reasons (i.e., poor solubility of the lithium base in 2-propanol) the latter experimental set-up is preferable. These observations indicate that the alkali ion also plays an intimate part in these reactions (see Mechanistic Considerations below).

Initial rate kinetics: To obtain further information on the different catalytic systems, additional experiments were performed. From the initial rate experiments, the effect of the different reaction components could be examined. Initially ketone concentrations were varied in the reactions catalyzed by either Rh–**3a** (thioamide) or Rh–**4a** (hydroxamic acid), whereas the other components were kept constant. The formation of 1-phenylethanol as a function of time was plotted for a series of different acetophenone concentrations using the following conditions: [Rh–**3a**] or [Rh–**4a**] = 0.001012 M, [$NaOPr^i$] = 0.009773 M, and [acetophenone] = 0.009773–0.3909 M in 2-propanol at a constant volume of 25.58 mL (Figure 4). It was found that the two catalytic systems behaved rather differently. In the case of the Rh–**3a**-catalyzed reduction, the reaction rate was linearly correlated with the ketone concentration and only at a high acetophenone concentration (0.39 M) was the substrate dependence found to be of decreasing importance. Conversely, when Rh–**4a** was employed as the catalyst, the initial rates were essentially equal regardless of the ketone concentration and only at low initial concentrations of acetophenone (< 0.1 M) did the reaction proceed at a lower rate. This behavior indicates pseudo-first-order reaction conditions in ketone for the thioamide-derived catalyst system. The Rh–**4a**-catalyzed reaction, on the other hand, demonstrates a pseudo-zero-order dependence on acetophenone.

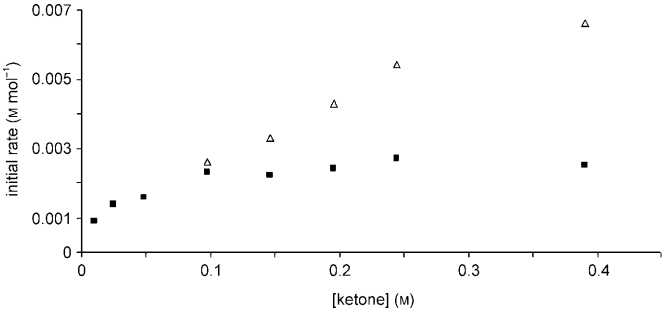

Figure 4. Initial reaction rates as a function of acetophenone concentration: △) Rh–**3a** and ■) Rh–**4a**.

Next, the effect of different 2-propanol concentrations on the initial rates of the ATH reaction of acetophenone was examined. By using the same reaction conditions as in the experiments presented above, but with a constant acetophenone concentration of 0.1955 M and a variation of the concentration of 2-propanol from 3–12.78 M with THF as co-solvent, the plots presented in Figure 5 were obtained. The results show that a first-order dependence on 2-propanol was found for both catalytic systems. However, at high 2-propa-

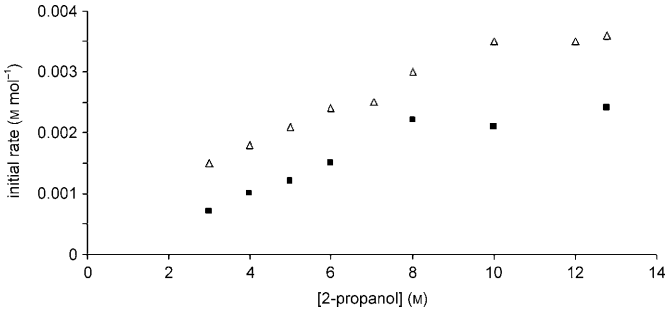

Figure 5. Initial reaction rates as a function of 2-propanol concentration: △) Rh–**3a** and ■) Rh–**4a**.

nol concentrations ([2-propanol] = 8–10 M), a saturation effect was noticed because the rates did not increase further.

At a first glance, the above results indicate that the two catalytic systems behave rather differently and that the individual processes might have different rate-determining steps. The direct correlation between acetophenone concentration and the initial rate suggests that ketone reduction is rate-limiting in the ATH reaction catalyzed by Rh–**3a**. In contrast, the pseudo-zero-order dependence on acetophenone concentration found for the reduction process employing Rh–**4a** suggests that rhodium hydride formation could be the rate-determining step. For a better description of the behavior of the two different catalytic systems, a more in depth analysis of the rate constants associated with the individual reaction steps was undertaken.

Determination of the rate constants: From the initial rate experiments it is possible to calculate the rate constants associated with the ATH reaction. The ATH reaction sequence with either of the two different catalysts Rh–**3a** and Rh–**4a** can be divided into two consecutive steps, the formation of the rhodium hydride followed by the reduction of the substrate (Scheme 1, steps 1 and 2, respectively).

The rate expressions for the individual steps can be described by Equations (1) and (2).

$$\text{rate}(1) = k_1[2-\text{propanol}][\text{Rh}] - k_{-1}[\text{acetone}][\text{Rh}-\text{H}] \quad (1)$$

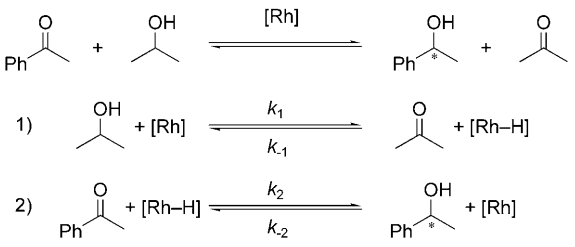

Scheme 1. Schematic representation of the individual reaction steps and the overall process for the rhodium-catalyzed ATH of acetophenone.

$$\text{rate}(2) = k_2[\text{acetophenone}][\text{Rh}-\text{H}] - k_{-2}[1-\text{phenylethanol}][\text{Rh}] \quad (2)$$

Because the total catalyst concentration remains constant throughout the reaction, the concentration of the individual rhodium species [Rh] and [Rh–H] can be expressed by Equation (3).

$$[\text{Rh}]_{\text{tot}} = [\text{Rh}] + [\text{Rh}-\text{H}] \quad (3)$$

Combining the above equations gives the overall rate expression [Eq. (4)] for the reaction.

$$\text{rate} = [\text{Rh}]_{\text{tot}}\left(\frac{k_1k_2[2-\text{propanol}][\text{acetophenone}] - k_{-1}k_{-2}[\text{acetone}][1-\text{phenylethanol}]}{k_1[2-\text{propanol}] + k_2[\text{acetophenone}] + k_{-1}[\text{acetone}] + k_{-2}[1-\text{phenylethanol}]}\right) \quad (4)$$

The magnitude of the individual rate constants associated with the different steps in the ATH process can be obtained from analyzing the results of reactions performed under different conditions (see the Supporting Information for further details).[20] The values of the individual rate constants obtained according to the initial rate analysis for the different catalytic systems, employing catalysts Rh–**3a** and Rh–**4a**, are presented in Table 4. An alternative to the use of the initial rate method is to study the complete reaction of the individual experiments and to model the obtained profiles for the determination of the individual rate constants (k_1, k_{-1}, k_2, and k_{-2}) in Equation (4). The experimental data for the reactions catalyzed by the hydroxamic acid derived complex (Rh–**4a**) were modeled by using the DynaFit software[21] in which a total of 257 data points were simultaneously fitted to give estimated values of k_1, k_{-1}, k_2, and k_{-2} (Table 4 and Figure 6). It was, however, not possible to obtain reliable modeled rate constants for the reaction catalyzed by the thioamide-derived complex Rh–**3a**. This finding can either be explained by the use of an incorrect mechanism in the simulation or by possible catalyst deactivation during the course of the reaction. To gain further understanding about the nature of the reaction catalyzed by complex Rh–**3a**, an experiment was performed in which the acetophenone was added to the mixture of all the other components with a delay of 1 h. The reaction profile and hence the rate of the reaction was found to be considerably different to those obtained under the standard conditions (Figure 7). From the curves and the initial rates obtained (4.3 mM min^{-1} under standard conditions and 2.9 mM min^{-1} with substrate addition after 1 h), it can be concluded that the catalyst is clearly affected over time. The latter finding suggests that the use of initial rate kinetics for studies on the Rh–**3a**-catalyzed system is preferable.

A comparison of the rate constants for the reaction catalyzed by complex Rh–**4a** (Table 4) shows that the calculated initial rates are in good agreement with the modeled ones representing the complete reaction. The magnitudes of k_1, k_{-1}, k_2, and k_{-2} are the same in both cases. Analysis of the magnitudes of the individual rate constants presented in Table 4 shows that the two catalyst systems operate rather

Table 4. Kinetic rate constants and calculated initial rates for the ATH reaction of acetophenone in 2-propanol catalyzed by [Rh–**3a**] and [Rh–**4a**].

	k_1 [$M^{-1}min^{-1}$]	k_{-1} [$M^{-1}min^{-1}$]	k_2 [$M^{-1}min^{-1}$]	k_{-2} [$M^{-1}min^{-1}$]	Initial rate of step 1[a] [$mM\,min^{-1}$]	Initial rate of step 2[a] [$mM\,min^{-1}$]
initial rate data for Rh–**3a**	1.12	100	31.3	2.69	14.5	6.18
initial rate data for Rh–**4a**	0.198	69.4	137	3.01	2.55	27.1
modeled data for Rh–**4a**	0.284 ± 0.0098	26.0 ± 2.8	62.2 ± 6.0	5.37 ± 0.45	3.67	12.3

[a] The initial rates were calculated by using Equations (5) and (6). Concentrations used in the calculations were [Rh] = 0.001012 M, [2-propanol] = 12.78 M, and [acetophenone] = 0.1955 M.

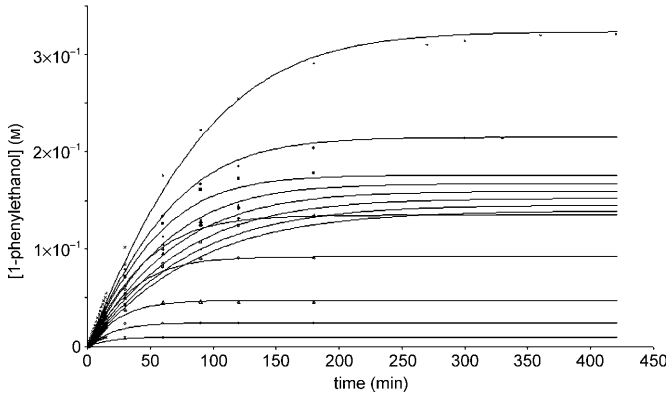

Figure 6. Modeled reaction profiles for the ATH reaction of acetophenone catalyzed by Rh–**4a**. The points represent experimental data and lines represent the modeled profiles.

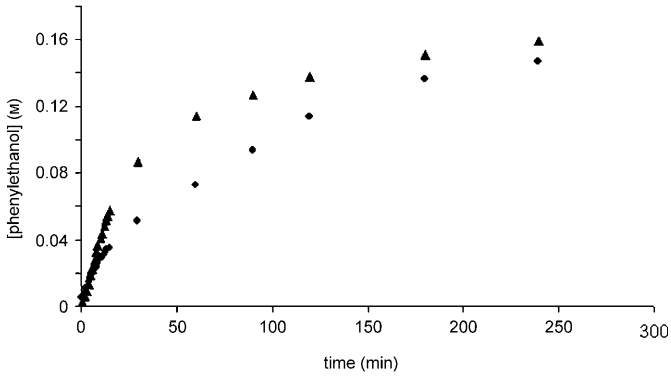

Figure 7. Reaction profiles as a function of time using catalyst Rh–**3a**: ▲) standard experiment and ●) substrate addition after 1 h.

differently. In the reaction catalyzed by the thioamide-containing catalyst Rh–**3a**, $k_{-1} > k_2$, which suggests that the transition state for the initial hydride-forming step is lower in energy than the second product-generating step. Conversely, in the reaction catalyzed by Rh–**4a**, k_{-1} is less than k_2. Hence, the energetically highest activation barrier for the hydroxamic acid containing catalyst is associated with the initial step. Furthermore, with the rate constants in hand it is possible to calculate the initial rates associated with the forward reactions of the individual reaction steps 1 and 2 presented in Scheme 1. At very low acetone and 1-phenylethanol concentrations, the initial rates for steps 1 and 2 are given by Equations (5) and (6).

$$\text{rate}(1) = k_1[\text{2-propanol}][\text{Rh}] \quad (5)$$

$$\text{rate}(2) = k_2[\text{acetophenone}][\text{Rh}] \quad (6)$$

Comparison of the initial rates obtained for the individual steps provides valuable information on the rate-determining step associated with the different processes. Hence, if $k_2[\text{acetophenone}] \ll k_1[\text{2-propanol}]$, step 2 becomes rate-limiting. On the other hand, if $k_2[\text{acetophenone}] \gg k_1[\text{2-propanol}]$, the hydride-generating step becomes rate-determining.

For the ATH reaction of acetophenone catalyzed by Rh–**4a**, the calculated rate for the hydride formation (step 1) was found to be 3.67 $mM\,min^{-1}$ at [acetophenone] = 0.1955 M, which is slightly lower than the hydride transfer to the substrate (step 2), for which the rate is 12.3 $mM\,min^{-1}$. These values suggest that, at an early stage of the reaction, the hydride formation (step 1) is rate-limiting. Conversely, in the reaction catalyzed by complex Rh–**3a**, the rate for hydride formation is substantially higher 14.5 $mM\,min^{-1}$. Moreover, the lower value for hydride transfer to the ketone (6.18 $mM\,min^{-1}$) indicates that the rate-determining step in the Rh–**3a**-catalyzed reaction is the second step. It can thus be concluded that the rate-determining step was different for the two catalyst systems, with the hydride formation being rate-limiting in the reaction catalyzed by the hydroxamic acid derived catalyst (step 1) and the hydride transfer to the substrate being rate-determining in the reaction catalyzed by the thioamides-derived catalyst (step 2).

Hammett plots: Competitive rate experiments with differently substituted acetophenones and with the parent ketone were performed. Plotting the logarithm of the relative rates against the Hammett σ values for the different substrates revealed, not surprisingly, that both catalyst systems display positive ρ values (Figure 8). The ρ values suggest that the reaction catalyzed by Rh–**3a** ($\rho = 2.66$, whereas $\rho = 1.99$ for Rh–**4a**) is slightly more sensitive to substrate substituent effects, a result that reflects the outcome of the initial rate study. The better linear fit should also be a consequence thereof.

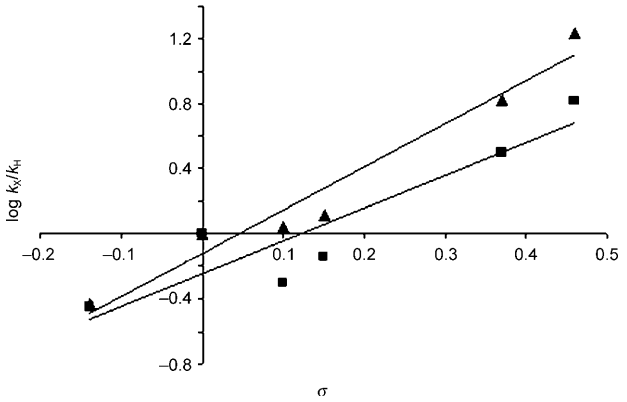

Figure 8. Hammett plot showing the effect of substituents on the transfer hydrogenation using different catalyst systems: ▲) Rh–**3a** and ■) Rh–**4a**.

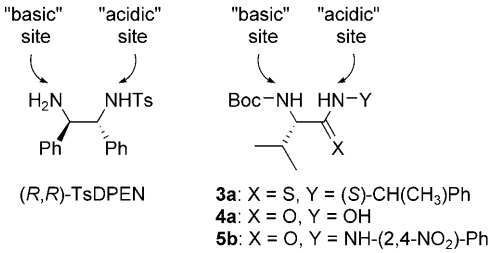

Figure 9. Structural resemblance between the TsDPEN and the amino acid derived ligands.

Mechanistic considerations: The mechanism of the asymmetric transfer hydrogenation using half-sandwich ruthenium or rhodium complexes with, in particular, the TsDPEN ligand has been extensively studied (i.e., the ATH reaction catalyzed by complex **1**).[22,23] It is generally accepted that the reaction proceeds by an outer-sphere mechanism in which the ketone substrate interacts with the bifunctional mono-hydride catalyst and simultaneously receives a hydride from the metal and a proton from the ligand. However, recent modeling studies of the transfer hydrogenation in solution indicate that solvent molecules play an important role in mediating proton transfers between the catalyst and the substrate.[24] The high enantioselectivity in the reduction of aryl alkyl ketones arises from a stabilizing electrostatic interaction (CH–π) between the arene ligand of the catalyst and the aryl ring of the substrate. Kinetic studies using the Noyori catalyst **1** in 2-propanol at high ketone concentration have revealed that the rate-determining step is the hydride formation/regeneration rather than the ketone reduction.[25] Because the metal in the catalyst complex becomes a stereogenic center upon hydride formation, two different diastereomeric complexes could theoretically be created. The excellent enantioselectivity obtained by using the Noyori catalyst implies that only one of the two possible isomers is formed. The amino acid based thioamide, hydroxamic acid, and hydrazide ligand systems show a large degree of structural resemblance with the TsDPEN ligand used in catalyst **1**. As depicted in Figure 9, all the ligand systems contain a basic and an acidic site, which are important for complex formation as well as catalytic activity. The acidic site in the TsDPEN ligand is evidently the sulfonamide and the corresponding site in the amino acid ligands is the C terminus. In the Noyori catalyst the amine acts as the basic site, whereas the corresponding site in the amino acid ligands is less obvious. From the structure–activity investigation presented above in which different functional groups were introduced at the ligand N terminus, we found that carbamates gave the best catalytic activity and selectivity. Therefore we can conclude that even if the carbamate as such is a poor base, the deprotonated form will be significantly more basic. Moreover, the stereochemical outcomes of the ATH reductions suggest that these ligands coordinate the metal in a bidentate fashion and, most importantly, with the amino acid part of the chelate ring.

The limited amount of structural information available on the catalytically active Ru/Rh complexes with either the pseudo-dipeptide or the amino acid based thioamide, hydroxamic acid, or hydrazide ligand systems drastically complicates the prediction of ligand coordination as well as the mechanistic analysis. The major difference between the ligand systems examined appears to be their mode of coordination. The isolated and characterized thioamide complex shown in Figure 2 displays catalytic properties that significantly deviate from what we obtain under standard reaction conditions. Therefore we can conclude that this complex is not the active catalyst operating in the reaction. Instead, the thioamides presumably interact with the metal through the carbamate nitrogen (or oxygen) and the thioamide sulfur atoms (**II** or **IV** of Figure 1). The hydroxamic acids, on the other hand, most probably coordinate the metal through the carbamate nitrogen (or oxygen) and the hydroxamic acid nitrogen atoms according to **VI** or **VIII** of Figure 1. The high enantioselectivity of either the *R* or the *S* isomer of the product alcohol obtained by using these complexes implies that two stereogenically different hydride complexes are responsible for product formation. Moreover, the difference in the rate-determining step demonstrated for the two catalytic systems further stresses a mechanistic divergence. As depicted in Scheme 2a, we suggest that the thioamide ligand **3a** interacts with the rhodium precursor to form a complex, which, upon reaction with 2-propanol, predominantly gives the (*S*)-ligand,(*S*)-rhodium (S_L,S_{Rh}) diastereomer. In agreement with the results obtained with catalyst **1**, the subsequent reaction with the substrate selectively gives the (*R*)-alcohol. The stereochemically opposite result obtained by using the rhodium catalyst derived from the hydroxamic acid **4a** suggests that the reduction of the ketone is mediated by the (*S*)-ligand,(*R*)-rhodium (S_L,R_{Rh}) complex (Scheme 2b). The pseudo-zero-order dependence on ketone concentration using Rh–**4a** suggests that the rate-limiting step is the metal hydride formation rather than the substrate reduction. Hence, once the (S_L,R_{Rh})-Rh–**4a** hydride is formed, a fast reaction with the substrate will lead to the formation of the *S* isomer of the product. The underlying reason why the rhodium complexes of ligands **3a** and **4a**

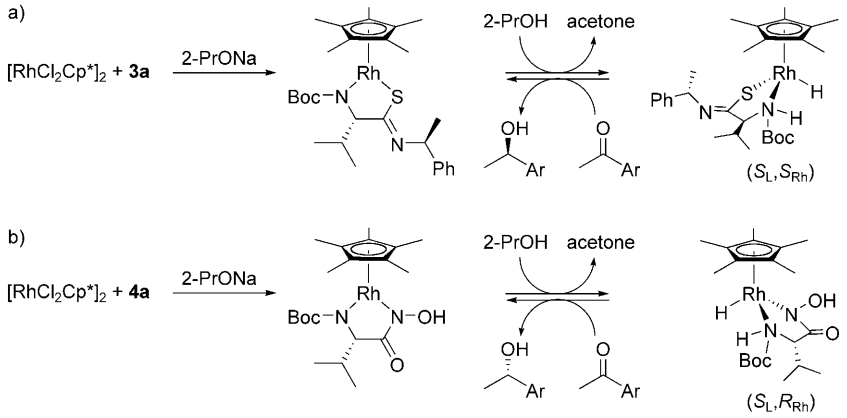

Scheme 2. Suggested rhodium hydride complexes formed with a) thioamide ligand **3a** and b) hydroxamic acid ligand **4a**.

will generate two different metal hydride diastereomers, even if they are based on the same amino acid scaffold, could be explained by secondary steric and/or electronic interactions between the substituents on the thioamide and the hydroxamic acid and the Cp* ligand. In addition, it is possible that the Rh–**3a** complex can undergo hydride formation with 2-propanol to yield both the (S_L,S_{Rh}) and the (S_L,R_{Rh}) hydride intermediates. Because the rate-determining step is the delivery of a hydride to the substrate, these two complexes can be in equilibrium with each other and the lowest barrier towards product formation is via the (S_L,S_{Rh}) intermediate (cf. Curtin–Hammett kinetics). The enhancement of activity and enantioselectivity observed upon addition of lithium chloride is difficult to explain, however, we assume that the Lewis acidic metal can interact with the substrate and the oxygen atom of the carbamate carbonyl in the hydride transfer step and thereby facilitate a highly organized transition state.

Conclusion

The rhodium-catalyzed asymmetric transfer hydrogenation of acetophenone using amino acid derived ligands containing thioamide and hydroxamic acid functionalities have been investigated to further our understanding of the observed enantioswitchable nature of these catalytic systems. The reduction of acetophenone using thioamide-containing ligands from naturally occurring amino acids selectively gave the (*R*)-alcohol (95% *ee*), whereas the use of the corresponding hydroxamic acid ligand system gave the *S* product with excellent enantioselectivity (97% *ee*). The structure–activity investigation performed on the thioamide and hydroxamic acid ligands revealed that subtle variations of the ligand structure caused dramatic effects on the reaction outcome. Replacing the N terminus of the ligands with groups other than carbamates resulted in a loss of catalytic activity and in most cases a significant decrease in the selectivity. Furthermore, an "acidic" proton at the C terminus was found to be crucial for the catalytic activity. Kinetic studies were carried out to examine the reaction order and we found that the hydroxamic acid based catalyst system Rh–**4a** showed pseudo-zero-order dependence on the substrate. Furthermore, the rate constants for the reactions were determined and from the overall kinetic data we concluded that the rate-limiting step for the reaction with the Rh–**4a** catalyst is the rhodium hydride formation. In contrast, the thioamide-derived catalyst system Rh–**3a** demonstrated pseudo-first-order kinetics with respect to ketone concentration. This observation, along with other kinetic data, is in accordance with the results reported for the Noyori catalyst system and implies that there is an interaction between the substrate and the catalyst in the rate-determining step. The absence of nonlinear behavior suggests that monomeric metal complexes are operating as catalysts in the ketone reductions. Thus, when all the results are summarized, we can conclude that the ligands most likely coordinate the metal in a bidentate fashion, with the amino acid part of the chelate ring. The origin of the ambivalent selectivity found by using the amino acid derived ligand classes can be traced to their different modes of coordination, along with differences in the reaction rates for product formation. The thioamides and hydroxamic acids share a common coordination site, namely, the carbamate nitrogen or possibly the oxygen atom. However, a difference is found at the "acidic" amino acid C terminus, the deprotonated thioamide ligand coordinating the metal through the sulfur atom and the corresponding hydroxamic acid ligand binding through the deprotonated hydroxy-amide nitrogen. The N−S coordination thus obtained with the thioamides results in a complex that favors ketone reduction by the (S_L,S_{Rh}) rhodium hydride. The transfer of a proton and a hydride from (S_L,S_{Rh})-Rh–**3a** to the *Si* face of the substrate facilitates the formation of the observed (*R*)-alcohol. The corresponding hydroxamic acid ligand, which coordinates the metal in an N−N fashion, should thereby favor the formation of the diastereomeric hydride isomer (S_L,R_{Rh}), which upon interaction with the substrate will form the opposite product enantiomer. In addition, we investigated the use of an additional ligand class derived from carbamate-protected amino acids, namely hydrazides. We found that the in situ formed rhodium complex based on the hydrazide ligand formed from *N*-Boc-valine and 2,4-dinitrophenylhydrazine catalyzed the reduction of acetophenone to give a moderate conversion and good enantioselectivity (91%). Catalysts based on the hydrazide ligands behaved in accordance with the hydroxamic acids and should coordinate the metal in a similar fashion.

Acknowledgements

The Swedish Research Council, the Knut and Alice Wallenberg Foundation, the Carl Trygger Foundation and the Wenner-Gren Foundation are gratefully acknowledged for financial support and postdoctoral fellowship (A.B.Z.).

[1] a) G. Zassinovich, G. Mestroni, S. Gladiali, *Chem. Rev.* **1992**, *92*, 1051; b) T. Ohkuma, R. Noyori in *Comprehensive Asymmetric Catalysis I-III, Vol. 1* (Eds.: E. N. Jacobsen, A. Pfaltz, H. Yamamoto), Springer, Berlin, **1999**, p. 199; c) H.-U. Blaser, C. Malan, B. Pugin, F. Spindler, H. Steiner, M. Studer, *Adv. Synth. Catal.* **2003**, *345*, 103; d) K. Everaere, A. Mortreux, J.-F. Carpentier, *Adv. Synth. Catal.* **2003**, *345*, 67; e) S. Gladiali, E. Alberico in *Transition Metals for Organic Synthesis, Vol. 2* (Eds.: M. Beller, C. Bolm), Wiley-VCH, Weinheim, **2004**, p. 145; f) A. Zanotti-Gerosa, W. Herns, M. Groarke, F. Hancock, *Platinum Met. Rev.* **2005**, *49*, 158; g) T. Ikariya, K. Murata, R. Noyori, *Org. Biomol. Chem.* **2006**, *4*, 393; h) R. Noyori, S. Hashiguchi, *Acc. Chem. Res.* **1997**, *30*, 97; i) C. Bianchini, L. Glendenning, *Chemtracts* **1997**, *10*, 333; j) M. J. Palmer, M. Wills, *Tetrahedron: Asymmetry* **1999**, *10*, 2045; k) T. Ohkuma, R. Noyori, *Compr. Asymmetric Catal. Suppl.* **2004**, *1*, 43; l) M. Kitamura, R. Noyori in *Ruthenium in Organic Synthesis* (Ed.: S.-I. Murahashi), Wiley-VCH, Weinheim, **2004**, p. 3; m) S. Gladiali, E. Alberico, *Chem. Soc. Rev.* **2006**, *35*, 226; n) T. Ikariya, K. Murata, R. Noyori, *Org. Biomol. Chem.* **2006**, *4*, 393; o) X. Wu, J. Xiao, *Chem. Commun.* **2007**, 2449; p) S. Gladiali, R. Taras in *Modern Reduction Methods* (Eds.: P. G. Andersson, I. Munslow), Wiley-VCH, Weinheim, **2008**, p. 135; q) C. Wang, X. Wu, J. Xiao, *Chem. Asian J.* **2008**, *3*, 1750.

[2] For recent selected examples, see: a) A. Schlatter, M. K. Kundu, W.-D. Woggon, *Angew. Chem.* **2004**, *116*, 6899; *Angew. Chem. Int. Ed.* **2004**, *43*, 6731; b) D. Xue, Y.-C. Chen, X. Cui, Q.-W. Wang, J. Zhu, J.-G. Deng, *J. Org. Chem.* **2005**, *70*, 3584; c) X. Wu, X. Li, F. King, J. Xiao, *Angew. Chem.* **2005**, *117*, 3473; *Angew. Chem. Int. Ed.* **2005**, *44*, 3407; d) A. M. Hayes, D. J. Morris, G. J. Clarkson, M. Wills, *J. Am. Chem. Soc.* **2005**, *127*, 7318; e) W. Baratta, G. Chelucci, S. Gladiali, K. Siega, M. Toniutti, M. Zanette, E. Zangrando, P. Rigo, *Angew. Chem.* **2005**, *117*, 6370; *Angew. Chem. Int. Ed.* **2005**, *44*, 6214; f) S. Enthaler, R. Jackstell, B. Hagemann, K. Junge, G. Erre, M. Beller, *J. Organomet. Chem.* **2006**, *691*, 4652; g) M. T. Reetz, X. Li, *J. Am. Chem. Soc.* **2006**, *128*, 1044.

[3] The use of primary diols as hydride donors, which result in irreversible reaction conditions, has recently been reported, see: H. C. Maytum, B. Tavassoli, J. M. J. Williams, *Org. Lett.* **2007**, *9*, 4387.

[4] H. Adkins, R. M. Elofson, A. G. Rossow, C. C. Robinson, *J. Am. Chem. Soc.* **1949**, *71*, 3622.

[5] a) H. Meerwein, R. Schmidt, *Justus Liebigs Ann. Chem.* **1925**, *444*, 221; b) M. Verley, *Bull. Soc. Chim. Fr.* **1925**, *37*, 871; c) W. Ponndorf, *Angew. Chem.* **1926**, *38*, 138; d) C. F. de Graauw, J. A. Peters, H. van Bekkum, J. Huskens, *Synthesis* **1994**, 1007; e) K. Nishide, M. Node, *Chirality* **2002**, *14*, 759.

[6] For recent examples of aluminium-mediated MPVO reactions, see: a) Y.-C. Liu, B.-T. Ko, B.-H. Huang, C.-C. Lin, *Organometallics* **2002**, *21*, 2066; b) T. Ooi, T. Miura, Y. Itagaki, H. Ichikawa, K. Maruoka, *Synthesis* **2002**, 279; c) T. Ooi, H. Ichikawa, K. Maruoka, *Angew. Chem.* **2001**, *113*, 3722; *Angew. Chem. Int. Ed.* **2001**, *40*, 3610.

[7] For a recent example of an efficient lithium-mediated MPVO process, see: J. Ekström, J. Wettergren, H. Adolfsson, *Adv. Synth. Catal.* **2007**, *349*, 1609.

[8] a) C. P. Casey, H. Guan, *J. Am. Chem. Soc.* **2007**, *129*, 5816; b) S. Enthaler, B. Hagemann, G. Erre, K. Junge, M. Beller, *Chem. Asian J.* **2006**, *1*, 598; c) S. Enthaler, G. Erre, M. Kin Tse, K. Junge, M. Beller, *Tetrahedron Lett.* **2006**, *47*, 8095.

[9] a) S. Hashiguchi, A. Fujii, J. Takahara, T. Ikariya, R. Noyori, *J. Am. Chem. Soc.* **1995**, *117*, 7562; b) A. Fujii, S. Hashiguchi, N. Uematsu, T. Ikariya, R. Noyori, *J. Am. Chem. Soc.* **1996**, *118*, 2521.

[10] a) D. A. Alonso, D. Guijarro, P. Pinho, O. Temme, P. G. Andersson, *J. Org. Chem.* **1998**, *63*, 2749; b) D. A. Alonso, S. J. Nordin, P. Roth, T. Tarnai, P. G. Andersson, M. Thommen, U. Pittelkow, *J. Org. Chem.* **2000**, *65*, 3116; c) S. J. Nordin, P. Roth, T. Tarnai, D. A. Alonso, P. Brandt, P. G. Andersson, *Chem. Eur. J.* **2001**, *7*, 1431; d) M. J. Palmer, T. Walsgrove, M. Wills, *J. Org. Chem.* **1997**, *62*, 5226; e) M. Wills, M. Gamble, M. J. Palmer, A. R. C. Smith, J. R. Studley, J. A. Kenny, *J. Mol. Catal. A* **1999**, *146*, 139; f) M. J. Palmer, J. A. Kenny, T. Walsgrove, A. M. Kawamoto, M. Wills, *J. Chem. Soc. Perkin Trans. 1* **2002**, 416; g) J. Takehara, S. Hashiguchi, A. Fujii, S. Inoue, T. Ikariya, R. Noyori, *J. Chem. Soc. Chem. Commun.* **1996**, 233.

[11] a) I. M. Pastor, P. Västilä, H. Adolfsson, *Chem. Commun.* **2002**, 2046; b) I. M. Pastor, P. Västilä, H. Adolfsson, *Chem. Eur. J.* **2003**, *9*, 4031; c) A. Bøgevig, I. M. Pastor, H. Adolfsson, *Chem. Eur. J.* **2004**, *10*, 294; d) P. Västilä, J. Wettergren, H. Adolfsson, *Chem. Commun.* **2005**, 4039; e) J. Wettergren, A. Bøgevig, M. Portier, H. Adolfsson, *Adv. Synth. Catal.* **2006**, *348*, 1277; f) P. Västilä, A. B. Zaitsev, J. Wettergren, T. Privalov, H. Adolfsson, *Chem. Eur. J.* **2006**, *12*, 3218; g) A. B. Zaitsev, H. Adolfsson, *Org. Lett.* **2006**, *8*, 5129; h) K. Ahlford, A. B. Zaitsev, J. Ekström, H. Adolfsson, *Synlett* **2007**, 2541; i) J. Wettergren, A. B. Zaitsev, H. Adolfsson, *Adv. Synth. Catal.* **2007**, *349*, 2556; j) L. Zani, L. Eriksson, H. Adolfsson, *Eur. J. Org. Chem.* **2008**, 4655.

[12] a) T. Ohta, S.-I. Nakahara, Y. Shigemura, K. Hattori, I. Furukawa, *Chem. Lett.* **1998**, 491; b) D. Carmona, F. J. Lahoz, R. Atencio, L. A. Oro, M. P. Lamata, F. Viguri, E. San José, C. Vega, J. Reyes, F. Joó, Á. Kathó, *Chem. Eur. J.* **1999**, *5*, 1544; c) Á. Kathó, D. Carmona, F. Viguri, C. D. Remacha, J. Kovács, F. Joó, L. A. Oro, *J. Organomet. Chem.* **2000**, *593*, 299; d) T. Ohta, S.-I. Nakahara, Y. Shigemura, K. Hattori, I. Furukawa, *Appl. Organomet. Chem.* **2001**, *15*, 699; e) J. W. Faller, A. R. Lavoie, *Organometallics* **2001**, *20*, 5245; f) H. Y. Rhyoo, Y. A. Yoon, H. J. Park, Y. K. Chung, *Tetrahedron Lett.* **2001**, *42*, 5045; g) H. Y. Rhyoo, H.-J. Park, Y. K. Chung, *Chem. Commun.* **2001**, 2064; h) D. Carmona, M. P. Lamata, F. Viguri, I. Dobrinovich, F. J. Lahoz, L. A. Oro, *Adv. Synth. Catal.* **2002**, *344*, 499; i) D. Carmona, J. Ferrer, E. Lalaguna, M. Lorenzo, F. J. Lahoz, S. Elipe, L. A. Oro, *Eur. J. Inorg. Chem.* **2002**, 259; j) H. Y. Rhyoo, H.-J. Park, W. H. Suh, Y. K. Chung, *Tetrahedron Lett.* **2002**, *43*, 269; k) P. Pelagatti, M. Carcelli, F. Calbiani, C. Cassi, L. Elviri, C. Pelizzi, U. Rizzotti, D. Rogolino, *Organometallics* **2005**, *24*, 5836; l) W. Hoffmueller, H. Dialer, W. Beck, *Z. Naturforsch. B* **2005**, *60*, 1278; m) P. Pelagatti, A. Bacchi, F. Calbiani, M. Carcelli, L. Elviri, C. Pelizzi, D. Rogolino, *J. Organomet. Chem.* **2005**, *690*, 4602.

[13] For a comprehensive overview of acidity constants, please see the following website: http://www.chem.wisc.edu/areas/reich/pkatable/index.htm.

[14] a) D. G. Blackmond, M. Ropic, M. Stefinovic, *Org. Process Res. Dev.* **2006**, *10*, 457; b) D. S. Matharu, D. J. Morris, A. M. Kawamoto, G. J. Clarkson, M. Wills, *Org. Lett.* **2005**, *7*, 5489; c) X. Wu, D. Vinci, T. Ikariya, J. Xiao, *Chem. Commun.* **2005**, 4447.

[15] a) E. Farkas, É. A. Enyedy, G. Micera, E. Garribba, *Polyhedron* **2000**, *19*, 1727; b) F. Hintermaier, S. Helding, L. B. Volodarsky, K. Sünkel, K. Polborn, W. Beck, *Z. Naturforsch. B* **1998**, *53*, 101; c) E. Farkas, H. Csóka, *J. Inorg. Biochem.* **2002**, *89*, 219; d) C. J. Milios, E. Manessi-Zoupa, S. P. Perlepes, A. Terzis, C. P. Raptopoulou, *Trans. Metal Chem.* **2002**, *27*, 864.

[16] $C_{28}H_{42}ClN_2O_2RhS$, $M_r = 609.06$, crystal size $0.05 \times 0.03 \times 0.01$ mm, monoclinic, $C2$, $a = 18636(18)$, $b = 9.410(10)$, $c = 19.132(9)$ Å, $\beta = 112.69(3)°$, volume $= 3095(5)$ Å^3, $Z = 4$, $\rho_{calcd} = 1.307$ g cm^{-3}, $\mu = 0.730$ mm^{-1}, synchrotron, $\lambda \approx 0.9083$ Å, $T = 100$ K, $2\theta_{max} = 60.58°$, $N_{measured} = 9168$, $N_{unique} = 2381$, $R_{int} = 0.1982$, $R, = 0.0696$, $wR = 0.1573$. The diffraction data were collected on beam-line I911-5 at the Swedish synchrotron facility MaxLab, Lund (Sweden). The data was obtained with a MARCCD diffractometer by using ϕ scans at a detector distance of 35 mm. The structure was solved by using standard structure invariant direct methods using SHELXS97 (G. M. Sheldrick, *Acta Crystallogr. Sect. A* **2008**, 112–122) and refined with full matrix least-squares calculations using SHELXL97 (G. M. Shel-

drick, SHELXL97, Program for the Refinement of Crystal Structures, University of Göttingen, Göttingen (Germany), **1994**). Anomalous dispersion correction terms for the used wavelength (0.9083 Å) were obtained from WCROMER (a) S. Brennan, http://www.ccp14.ac.uk/ccp/ccp14/ftp-mirror/cross-section-sfac/pub/cross-section_codes/; b) L. Kissel, R. H. Pratt, *Acta Crystallogr. Sect. A* **1990**, *46*, 170–175).

[17] CCDC 712178 contains the supplementary crystallographic data for this paper. These data can be obtained free of charge from The Cambridge Crystallographic Data Centre via www.ccdc.cam.ac.uk/data_request/cif.

[18] R. L. Chowdhury, J.-E. Bäckvall, *J. Chem. Soc. Chem. Commun.* **1991**, 1063.

[19] For a recent discussion on the influence of base in ruthenium-catalyzed transfer hydrogenations, see: W. Baratta, K. Siega, P. Rigo, *Chem. Eur. J.* **2007**, *13*, 7479.

[20] J. Wettergren, E. Buitrago, P. Ryberg, H. Adolfsson, *Chem. Eur. J.* **2009**, *15*, 5709.

[21] P. Kuzmic, *Anal. Biochem.* **1996**, *237*, 260.

[22] a) M. Yamakawa, I. Yamada, R. Noyori, *Angew. Chem.* **2001**, *113*, 2900; *Angew. Chem. Int. Ed.* **2001**, *40*, 2818; b) R. Noyori, M. Yamakawa, S. Hashiguchi, *J. Org. Chem.* **2001**, *66*, 7931; c) M. Yamakawa, H. Ito, R. Noyori, *J. Am. Chem. Soc.* **2000**, *122*, 1466; d) D. A. Alonso, P. Brandt, S. J. M. Nordin, P. G. Andersson, *J. Am. Chem. Soc.* **1999**, *121*, 9580; e) P. Brandt, P. Roth, P. G. Andersson, *J. Org. Chem.* **2004**, *69*, 4885.

[23] For an excellent review on hydrogen transfer mechanisms, see: J. S. M. Samec, J.-E. Bäckvall, P. G. Andersson, P. Brandt, *Chem. Soc. Rev.* **2006**, *35*, 237.

[24] J.-W. Handgraaf, E. J. Meijer, *J. Am. Chem. Soc.* **2007**, *129*, 3099.

[25] a) K. J. Haack, S. Hashiguchi, A. Fujii, T. Ikariya, R. Noyori, *Angew. Chem.* **1997**, *109*, 297; *Angew. Chem. Int. Ed. Engl.* **1997**, *36*, 285; b) F. K. Cheung, C. Lin, F. Minissi, A. L. Crivillé, M. A. Graham, D. J. Fox, M. Wills, *Org. Lett.* **2007**, *9*, 4659.

Received: February 27, 2009
Revised: July 15, 2009
Published online: September 11, 2009

